

Photon counting for axion interferometry

Haocun Yu

*University of Vienna, Faculty of Physics,
Vienna Center for Quantum Science and Technology (VCQ),
Boltzmannngasse 5, A-1090, Vienna, Austria.*

Ohkyung Kwon

University of Chicago, Chicago, Illinois 60637, USA.

Hartmut Grote

School of Physics and Astronomy, Cardiff University, Cardiff CF24 3AA, United Kingdom.

Denis Martynov

University of Birmingham, School of Physics and Astronomy, Birmingham B15 2TT, United Kingdom.

Axions and axion-like particles are well-motivated dark matter candidates. We propose an experiment that uses single photon detection interferometry to search for axions and axion-like particles in the galactic halo. We show that photon counting with a dark rate of 6×10^{-6} Hz can improve the quantum sensitivity of axion interferometry by a factor of 50 compared to the quantum-enhanced heterodyne readout for 5-m long optical resonators. The proposed experimental method has the potential to be scaled up to kilometer-long facilities, enabling the detection or setting of constraints on the axion-photon coupling coefficient of $10^{-17} - 10^{-16}$ GeV $^{-1}$ for axion masses ranging from 0.1 to 1 neV.

I. INTRODUCTION

The existence of dark matter has been overwhelmingly suggested by substantial evidence from astrophysical [1–3] and cosmological observations [4]. Among various extended theories beyond the Standard Model of particle physics, QCD axions [5–8] and pseudoscalar axion-like particles (ALPs) [9–11] are widely recognized as leading candidates.

We consider ALP dark matter to behave as a coherent, classical field a , and interact weakly with photons through the coefficient $g_{a\gamma}$:

$$\mathcal{L} \subset -\frac{1}{4}g_{a\gamma}aF\tilde{F}. \quad (1)$$

This interaction induces a phase velocity difference between left- and right-handed circularly polarized light, which can be accumulated and extracted using a properly designed optical cavity and laser interferometry [12–14].

Several experiments were proposed in the literature to search for ALPs with interferometry [13, 15] and the first results were recently published [16, 17]. In previous work, the signal light is measured by beating the signal field with a strong local oscillator field. The advantage of this technique is that the measurement can be done with a standard photodetector with a high quantum efficiency. However, the readout suffers from quantum shot noise from the local oscillator field.

In this paper, we derive the sensitivity of axion interferometers using photon-counting detectors and show their capacity to enhance detector sensitivity for axion fields with a short coherence time, compared to the periods between dark clicks of single photon detectors.

Over the past few decades, the technology for detecting single photons at near-infrared wavelengths has matured significantly [18, 19]. The idea of employing single photon detection was also introduced in the context of microwave cavity axion searches [20] and high-power interferometers for gravitational-wave detection [21]. Recent transition-edge sensors and superconducting nanowire single photon detectors (SNSPD) feature high detection efficiency exceeding 90% and exceptionally low dark count rates of 6×10^{-6} Hz [22–24]. These detectors would extend the time intervals between detector dark clicks, surpassing the coherence time of the axion field above 0.1 neV, and hold the potential to enhance the quantum-limited sensitivity of axion interferometers.

We hereby analyse an axion interferometer which consists of a linear optical cavity and derive its optimal parameters for heterodyne and single photon readouts. Our technique is also applicable to folded cavities. We calculate the signal-to-noise ratio for linear cavities of length from 1 m up to 10 km and show the advantage of single photon detection compared to heterodyne readout in axion interferometry. The proposed approach has the potential to be integrated into both table-top experiments and existing facilities for gravitational-wave detectors, such as GEO 600 [25] and LIGO facilities [26, 27].

II. EXPERIMENTAL SETUP

Figure 1 shows the proposed axion interferometer with single photon detection. A laser beam in P-polarisation (red) is injected into a high-finesse Fabry-Pérot linear cavity. To maximize the signal-to-noise

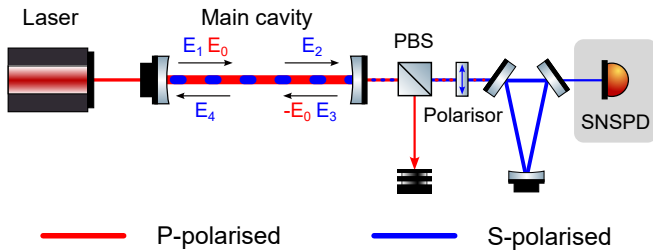


FIG. 1. **Schematic of the experimental setup.** P-polarised pump light resonates in a main linear optical cavity. The ALP field converts a small portion of light into S-polarised at a shifted frequency, which is isolated by a series of polarised optics and triangular optical cavities. The signal field is detected by a superconducting nanowire single photon detector (SNSPD). PBS: polarising beam splitter.

ratio, the bandwidth of this main cavity is designed to match one of the axion fields. It is also beneficial to keep the cavity undercoupled ($T_2 \gg T_1$) to transmit most of the signal field to the readout port, where T_1 and T_2 are transmissivities of the input and output coupler of the cavity. Due to the presence of the ALP field, the resonating laser field in P-polarisation undergoes partial conversion to S-polarisation (blue). The signal field around the free-spectral-range of the cavity is further amplified by the optical resonance and transmitted through the output port.

When using the method of heterodyne readout, a small fraction of the pump field is converted to S-polarisation and used as a local oscillator for the readout [28]. For the proposed single photon readout, the main challenge in the experiment is isolating S-polarisation photons from the P-polarisation ones in the pump field transmitting out of the cavity. The transmitted pump field has a photon rate of approximately 10^{20} Hz, which needs to be reduced to below 10^{-6} Hz to prevent false detections by the single photon readout.

Because the pump and signal fields have orthogonal polarisations, a series of polarised optics, including polarising beam splitters and linear polarisers with high extinction performance, can be used to reduce the transmitted pump field by up to 18 orders of magnitude. Due to imperfections in the polarisation optics, further suppression of the pump field is necessary. Since we are searching for axions at frequencies around the free-spectral-range of the main cavity, the signal fields are separated from the pump field in frequency as well. Accordingly, a series of triangular optical cavities with non-degenerate polarisation modes can serve as both frequency and polarisation filters for final signal extraction. These cavities can be controlled with auxiliary laser beams [29–31], and they need to have a bandwidth of $1/1000$ of the axion frequency and a high finesse to ensure a strong suppression of the pump field by up to factor of 8. Finally, an SNSPD with a low dark count rate, enclosed in a cryostat, is used for signal detection.

III. SENSITIVITY & INTEGRATION TIME

In this section, we show how single photon detectors can improve the sensitivity of axion interferometers. In our experiment, the observable quantity is the phase difference accumulated by the left- and right-handed circularly polarised light that propagates in the presence of the axion field for a time period τ . In SI units, the phase difference is given by the equation

$$\Delta\phi(t, \tau) = \sqrt{\hbar c} g_{a\gamma} [a(t) - a(t - \tau)], \quad (2)$$

where \hbar is the Planck constant, c is the speed of light, and $a(t)$ is the time-dependent amplitude of the axion field in the galactic halo.

Now, we consider how linearly polarised light propagates in the axion field between two points separated by a distance L . We adopt Jones calculus with the electric field vector given by $(E_p, E_s)^T$, where E_p and E_s are the horizontal and vertical components of the field. The Jones matrix for the propagation of light in the axion field is given by the equation

$$A^{-1} \begin{pmatrix} e^{i\Delta\phi/2} & 0 \\ 0 & e^{-i\Delta\phi/2} \end{pmatrix} A \approx \begin{pmatrix} 1 & \Delta\phi/2 \\ -\Delta\phi/2 & 1 \end{pmatrix}, \quad (3)$$

where matrices A and its inverse A^{-1} convert electric fields from the linear basis to circular ones and back.

In further analysis, we neglect the time dependence of the pump field in the cavity $E_{s,\text{cav}}$ because it is not affected by the axion field. The field in the S-polarisation builds up in the main cavity due to the axion field according to the equations

$$\begin{aligned} E_2(t) &= E_1(t - \tau) - \frac{1}{2}\Delta\phi(t, \tau)E_0, \\ E_3(t) &= r_2 E_2(t), \\ E_4(t) &= E_3(t - \tau) + \frac{1}{2}\Delta\phi(t, \tau)E_0, \\ E_1(t) &= r_1 E_4(t), \end{aligned} \quad (4)$$

where τ is the single-trip travel time in the cavity; r_1 and r_2 are the field reflectivities of the input and output couplers; E_0 is the pump field forward-propagating within the main linear cavity, with its sign flipped by the output coupler; E_{1-4} are S-polarisation electric fields propagating within the cavity near the input (E_1 and E_4) and output (E_2 and E_3) couplers (see Fig. 1). Solving Eq. (4) relative to E_1 , we get

$$E_1(t) = r_1 r_2 E_1(t - 2\tau) + \frac{E_0}{2} (\Delta\phi(t, \tau) - \Delta\phi(t - \tau, \tau)). \quad (5)$$

If dark matter consists of ALPs with mass m_a , then its field behaves classically and can be written as [32]:

$$a(t) = a_0 \sin(\Omega_a t + \delta(t)), \quad (6)$$

where the angular frequency $\Omega_a = 2\pi f_a = m_a c^2 / \hbar$ in SI units; $a_0 = \sqrt{2\rho_{\text{DM}} \hbar} / m_a$ is the amplitude of the field,

with $\rho_{\text{DM}} \approx 5.3 \times 10^{-22} \text{ kg/m}^3$ as the local density of dark matter; $\delta(t)$ is the phase of the field. The phase remains constant for times $t \lesssim \tau_a$, where $\tau_a = Q_a/f_a$ is the coherence time of the field, $Q_a = c^2/v^2 \sim 10^6$ is the quality factor of the oscillating field, and v is the galactic virial velocity of the ALP dark matter [9]. Eq. (6) neglects spacial variations of the field since ALPs wavelength $\lambda_a > 100 \text{ km}$ is significantly larger than the length of the proposed experiment for $m_a < 10^{-8} \text{ eV}$.

By setting the cavity single trip time to $\Omega_a \tau = \pi$ and applying Eq. (2) and (6), Eq. (5) can be simplified to

$$E_1(t) = r_1 r_2 E_1(t - 2\tau) + 2E_0 a(t) g_{a\gamma} \sqrt{\hbar c}. \quad (7)$$

Since the phase of the axion field stays constant much longer than τ , the solution for the field transmitted to the readout port is given by the equation

$$\begin{aligned} E_{\text{out}}(t) &= \sqrt{T_2} E_1(t) \approx E_0 \frac{\sqrt{T_2}}{1 - r_1 r_2} 2a(t) g_{a\gamma} \sqrt{\hbar c} \\ &\approx E_0 G \theta(t), \end{aligned} \quad (8)$$

where G represents the cavity gain, $\theta \ll 1$ is the conversion efficiency of the pump field to the signal field in the presence of the axion field.

We now consider the signal-to-noise ratio accumulated with two types of readout methods: heterodyne and single photon counting. For the heterodyne readout, we intend to install a half-wave plate in the transmission path of the cavity to convert a fraction of the transmitted pump field to the local oscillator field E_{LO} [15, 28]. The time-dependent component of the power observed on a photodetector is then given by the equation

$$P_h(t) = 2E_{\text{LO}} E_{\text{out}}(t) = 2\sqrt{P_{\text{LO}} P_0} G \theta(t). \quad (9)$$

The power spectral density of $P(t)$ around the frequency of the axion field Ω_a is given by the equation

$$S_{PP} = 16P_{\text{LO}} P_0 G^2 \frac{g_{a\gamma}^2 \rho_{\text{DM}} \hbar c^5}{\Omega_a^2} T, \quad (10)$$

where $T = \min(T_{\text{int}}, \tau_a)$ and $T_{\text{int}} \gg 1/\tau$ is the integration time. For $T_{\text{int}} < \tau_a$, we set our frequency spacing in the power spectral density estimation to $1/T_{\text{int}}$ and the peak in S_{PP} at frequency Ω_a grows linearly with time. For $T_{\text{int}} \geq \tau_a$, the peak of the axion field is resolved and the power spectral density does not grow for a larger integration time. However, the signal-to-noise ratio still improves for $T_{\text{int}} \geq \tau_a$ because we can subtract the mean value of the shot noise with higher precision. The power spectral density of the shot noise is given by the equation

$$S_{\text{shot}} = \frac{2\hbar\omega_0 P_{\text{LO}} e^{-2r}}{\sqrt{K}}, \quad (11)$$

where ω_0 is the angular frequency of the laser light; r is the squeezing factor [33, 34]; $K = \max(1, T_{\text{int}}/\tau_a)$ is the number of power spectral density averages that can be

made with a frequency resolution of $1/T_{\text{int}}$ for $T_{\text{int}} < \tau_a$, or with a resolution of $1/\tau_a$ for $T_{\text{int}} \geq \tau_a$. The signal-to-noise ratio is then given by the equation

$$\text{SNR}_h^2 = \frac{S_{PP}}{S_{\text{shot}}} = \frac{4P_0 G^2 g_{a\gamma}^2 \rho_{\text{DM}} c^4 \lambda e^{2r}}{\pi \Omega_a^2} \sqrt{T_{\text{int}} T}, \quad (12)$$

where λ is the wavelength of light.

In the case of photon counting, we observe only signal fields by rejecting the pump field in the orthogonal direction with polarisation optics and mode cleaners as discussed in Sec. II. The time-averaged power on the single photon detector is then given by the equation

$$P_c = P_0 G^2 g_{a\gamma}^2 \frac{4\rho_{\text{DM}} \hbar c^5}{\Omega_a^2}, \quad (13)$$

and the time-averaged number of photons observed during the integration time T_{int} is given by the equation

$$N = \frac{P_c T_{\text{int}}}{\hbar\omega_0} = P_0 G^2 g_{a\gamma}^2 \frac{2\rho_{\text{DM}} c^4 \lambda}{\pi \Omega_a^2} T_{\text{int}}, \quad (14)$$

We do not suffer from shot noise from the local oscillator while counting photons. However, single photon detectors observe dark counts with a time constant τ_d . For state-of-the-art single photon detectors, τ_d is in the order of 10^5 sec . If integration time $T_{\text{int}} = Q\tau_d$, we expect Q dark clicks of our detector with the standard deviation of \sqrt{Q} . Therefore, the signal-to-noise ratio is given by the equation

$$\text{SNR}_c^2 = \frac{N}{\sqrt{Q}} = \frac{2P_0 G^2 g_{a\gamma}^2 \rho_{\text{DM}} c^4 \lambda}{\pi \Omega_a^2} \sqrt{T_{\text{int}} T_d}, \quad (15)$$

where $T_d = \min(T_{\text{int}}, \tau_d)$.

Comparing the signal-to-noise ratios from Eq. (12) and Eq. (15), we find that an improvement in the estimation of $g_{a\gamma}$ can be achieved if $\tau_d \ll \tau_a$. The improvement factor is given by the equation

$$\frac{\text{SNR}_c}{\text{SNR}_h} = \frac{1}{\sqrt{2}e^r} \left(\frac{\tau_d}{\tau_a} \right)^{1/4} \approx \frac{1}{\sqrt{2}e^r} \left(\frac{\tau_d f_a}{Q_a} \right)^{1/4} \quad (16)$$

Fig. 2 compares the limits on $g_{a\gamma}$ that linear cavities can achieve with heterodyne (blue) and photon counting detectors (red). The cavity length is tuned for each frequency of the axion field $f_a = c/2L$ to satisfy the condition $\Omega_a \tau = \pi$. Based on the 5-m long LIDA detector with 120 kW resonating power [17], we assume the transmissivity of the cavity output coupler $T_2 = T_1 + Y$, where $Y = 1.7 \text{ ppm} \times \sqrt{L/5\text{m}}$ is the round-trip loss in a cavity of length L . We also impose $T_2 > 3 \text{ ppm}$ to ensure that the cavity bandwidth is larger than the bandwidth of the axion field. We assume the resonating power of $P_0 = \min(120 \text{ kW} \times L/5\text{m}, 10 \text{ MW})$. Since the beam size increases with the cavity length, the laser intensity on the mirrors stays the same when the cavity length and the resonating power are increased by

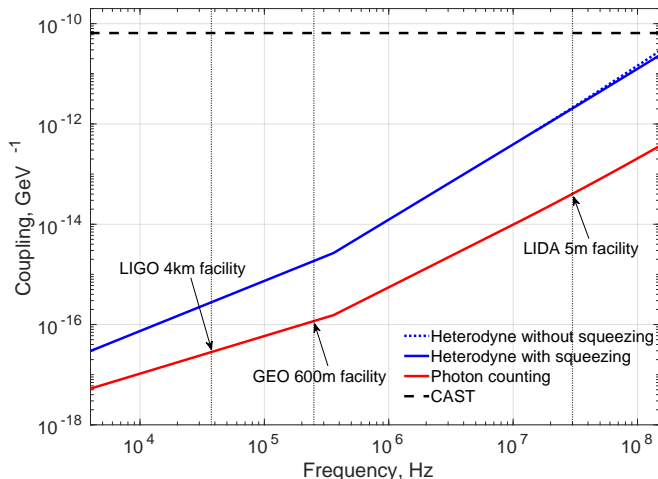


FIG. 2. Estimated limits on the axion-photon coupling coefficients using photon counting readout, compared with those obtained through heterodyne readout, with the CERN Axion Solar Telescope (CAST) as a reference.

the same factor. The upper limit of 10 MW is chosen to accommodate the technical complexities associated with maintaining high-quality coatings over large surface areas. For heterodyne readout, we assume the injection of 10 dB squeezing when the cavity is less than 10 m for quantum enhancement [28]. For photon counting, we assume an integration time T_{int} of 100 days and $\tau_d = 1.5 \times 10^5$ sec.

Taking the 5-m LIDA detector as an example, an improvement factor of 50 can be achieved with photon counting compared to the heterodyne readout when measuring $g_{a\gamma}$ at 30 MHz ($m_a = 124$ neV). The length of the GEO 600 facility corresponds to an axion frequency of 250 kHz ($m_a = 1$ neV), resulting in an improvement factor of 16. For a 4-km detector that can be installed in the LIGO facilities, the improvement factor would be 10 for an axion frequency of 37.5 kHz ($m_a = 0.15$ neV).

We also note that the sensitivity curves in Fig. 2 are calculated for a light wavelength $\lambda = 1064$ nm. Since Eq. (15) shows that the scaling of the signal-to-noise ratio scales as $\text{SNR} \sim \sqrt{\lambda}$ then the reduction of wavelength leads to an improvement on the $g_{a\gamma}$ constrains. Particularly, a 5-m long GHz resonator, similar to the ADMX one, and a qubit (two-level system)

operating as a single microwave photon detector [35] has the potential to probe axion fields around 100 neV down to $g_{a\gamma} \approx 10^{-16}$ GeV $^{-1}$.

IV. CONCLUSION

In this work, we proposed an axion interferometer with single photon counting methods targeting to detect or set constraints for axion-photon coupling coefficient for axion masses of 0.1 – 100 neV. Looking into the future, current gravitational-wave facilities are potential infrastructures to be transformed into axion interferometers, given their existing high-power lasers, ultra-stable linear optical cavities, and vacuum envelopes.

The key challenge of separating the pump field from the signal field can be approached by installing polarisation optics and a set of mode cleaners on the readout path. We also note that the sensitivity of the axion interferometer with photon readout is limited by the dark rate of state-of-the-art single photon detectors. Anticipated advancements in single photon detector technologies will lead to enhanced constraints on the parameter $g_{a\gamma}$.

Finally, we computed the sensitivity curve for both heterodyne and single-photon readout across resonator lengths ranging from 1 m to 10 km. The scaling of the SNR improvement will be similar for folded resonators as long as the dark count rate is larger than the bandwidth of the axion field. The scaling is also applicable for GHz resonators, which have the potential to probe the axion-photon interaction at a deeper level than constraining $g_{a\gamma}$ with optical resonators.

ACKNOWLEDGMENTS

We wish to acknowledge the support of the Quantum Interferometry collaboration for useful discussions. H. Yu acknowledges support from the Marie-Sklodowska Curie Postdoctoral Fellowship program, hosted by the Horizon Europe. D.M. acknowledges the support of the Institute for Gravitational Wave Astronomy at the University of Birmingham and STFC Quantum Technology for Fundamental Physics scheme (Grant No. ST/T006609/1 and ST/W006375/1). D.M. is supported by the 2021 Philip Leverhulme Prize.

[1] Y. Sofue and V. Rubin, Rotation curves of spiral galaxies, *Annual Review of Astronomy and Astrophysics* **39**, 137 (2001).
 [2] M. Markevitch, A. H. Gonzalez, D. Clowe, A. Vikhlinin, W. Forman, C. Jones, S. Murray, and W. Tucker, Direct constraints on the dark matter self-interaction cross section from the merging galaxy cluster 1e 0657-56, *The*

Astrophysical Journal **606**, 819 (2004).
 [3] R. Massey, T. Kitching, and J. Richard, The dark matter of gravitational lensing, *Reports on Progress in Physics* **73**, 086901 (2010).
 [4] G. Bertone, D. Hooper, and J. Silk, Particle dark matter: evidence, candidates and constraints, *Physics Reports* **405**, 279 (2005).

- [5] R. D. Peccei and H. R. Quinn, CP conservation in the presence of pseudoparticles, *Phys. Rev. Lett.* **38**, 1440 (1977).
- [6] J. Preskill, M. B. Wise, and F. Wilczek, Cosmology of the Invisible Axion, *Phys. Lett. B* **120**, 127 (1983).
- [7] L. F. Abbott and P. Sikivie, A Cosmological Bound on the Invisible Axion, *Phys. Lett. B* **120**, 133 (1983).
- [8] M. Dine and W. Fischler, The Not So Harmless Axion, *Phys. Lett. B* **120**, 137 (1983).
- [9] P. W. Graham and S. Rajendran, New observables for direct detection of axion dark matter, *Physical Review D* **88**, 10.1103/physrevd.88.035023 (2013).
- [10] A. Ringwald, Exploring the role of axions and other wisps in the dark universe, *Physics of the Dark Universe* **1**, 116 (2012), next Decade in Dark Matter and Dark Energy.
- [11] P. Svrcek and E. Witten, Axions in string theory, *Journal of High Energy Physics* **2006**, 051 (2006).
- [12] A. C. Melissinos, Proposal for a search for cosmic axions using an optical cavity, *Phys. Rev. Lett.* **102**, 202001 (2009).
- [13] W. DeRocco and A. Hook, Axion interferometry, *Physical Review D* **98**, 10.1103/physrevd.98.035021 (2018).
- [14] I. Obata, T. Fujita, and Y. Michimura, Optical ring cavity search for axion dark matter, *Physical Review Letters* **121**, 10.1103/physrevlett.121.161301 (2018).
- [15] H. Liu, B. D. Elwood, M. Evans, and J. Thaler, Searching for axion dark matter with birefringent cavities, *Phys. Rev. D* **100**, 023548 (2019).
- [16] Y. Oshima, H. Fujimoto, J. Kume, S. Morisaki, K. Nagano, T. Fujita, I. Obata, A. Nishizawa, Y. Michimura, and M. Ando, First results of axion dark matter search with dance (2023), arXiv:2303.03594 [hep-ex].
- [17] J. Heinze, A. Gill, A. Dmitriev, J. Smetana, T. Yan, V. Boyer, D. Martynov, and M. Evans, First results of the Laser-Interferometric Detector for Axions (LIDA) (2023), arXiv:2307.01365 [astro-ph.CO].
- [18] M. Eisaman, J. Fan, A. Migdall, and S. Polyakov, Invited review article: Single-photon sources and detectors, *The Review of scientific instruments* **82**, 071101 (2011).
- [19] I. Esmail Zadeh, J. Chang, J. Los, S. Gyger, A. W. Elshaari, S. Steinhauer, S. Dorenbos, and V. Zwiller, Superconducting nanowire single-photon detectors: A perspective on evolution, state-of-the-art, future developments, and applications, *Applied Physics Letters* **118**, 190502 (2021).
- [20] S. K. Lamoreaux, K. A. van Bibber, K. W. Lehnert, and G. Carosi, Analysis of single-photon and linear amplifier detectors for microwave cavity dark matter axion searches, *Phys. Rev. D* **88**, 035020 (2013).
- [21] L. McCuller, Single-photon signal sideband detection for high-power michelson interferometers (2022), arXiv:2211.04016 [physics.ins-det].
- [22] F. Marsili, V. B. Verma, J. A. Stern, S. Harrington, A. E. Lita, T. Gerrits, I. Vayshenker, B. Baek, M. D. Shaw, R. P. Mirin, and S. W. Nam, Detecting single infrared photons with 93% system efficiency, *Nature Photonics* **7**, 210 (2013).
- [23] D. V. Reddy, R. R. Nerem, S. W. Nam, R. P. Mirin, and V. B. Verma, Superconducting nanowire single-photon detectors with 98% system detection efficiency at 1550 nm, *Optica* **7**, 1649 (2020).
- [24] V. Verma, B. Korzh, A. Walter, A. Lita, R. Briggs, M. Colangelo, Y. Zhai, E. Wollman, A. Beyer, J. Allmaras, H. Vora, D. Zhu, E. Schmidt, A. Kozorezov, K. Berggren, R. Mirin, S. Nam, and M. Shaw, Single-photon detection in the mid-infrared up to 10 um wavelength using tungsten silicide superconducting nanowire detectors, *APL Photonics* **6**, 056101 (2021).
- [25] H. Grote and (the LIGO Scientific Collaboration), The GEO 600 status, *Classical and Quantum Gravity* **27**, 084003 (2010).
- [26] B. P. Abbott *et al.*, LIGO: the Laser Interferometer Gravitational-Wave Observatory, *Reports on Progress in Physics* **72**, 076901 (2009).
- [27] B. P. Abbott *et al.* (LIGO Scientific Collaboration and Virgo Collaboration), GW150914: The Advanced LIGO Detectors in the Era of First Discoveries, *Phys. Rev. Lett.* **116**, 131103 (2016).
- [28] D. Martynov and H. Miao, Quantum-enhanced interferometry for axion searches, *Phys. Rev. D* **101**, 095034 (2020).
- [29] A. Staley, D. Martynov, R. Abbott, R. X. Adhikari, K. Arai, S. Ballmer, L. Barsotti, A. F. Brooks, R. T. DeRosa, S. Dwyer, A. Effler, M. Evans, P. Fritschel, V. V. Frolov, C. Gray, C. J. Guido, R. Gustafson, M. Heintze, D. Hoak, K. Izumi, K. Kawabe, E. J. King, J. S. Kissel, K. Kokeyama, M. Landry, D. E. McClelland, J. Miller, A. Mullavey, B. O'Reilly, J. G. Rollins, J. R. Sanders, R. M. S. Schofield, D. Sigg, B. J. J. Slagmolen, N. D. Smith-Lefebvre, G. Vajente, R. L. Ward, and C. Wipf, Achieving resonance in the Advanced LIGO gravitational-wave interferometer, *Classical and Quantum Gravity* **31**, 245010 (2014).
- [30] K. Izumi, K. Arai, B. Barr, J. Betzwieser, A. Brooks, K. Dahl, S. Doravari, J. C. Driggers, W. Z. Korth, H. Miao, J. Rollins, S. Vass, D. Yeaton-Massey, and R. X. Adhikari, Multicolor cavity metrology, *J. Opt. Soc. Am. A* **29**, 2092 (2012).
- [31] A. J. Mullavey, B. J. J. Slagmolen, J. Miller, M. Evans, P. Fritschel, D. Sigg, S. J. Waldman, D. A. Shaddock, and D. E. McClelland, Arm-length stabilisation for interferometric gravitational-wave detectors using frequency-doubled auxiliary lasers, *Opt. Express* **20**, 81 (2012).
- [32] D. Budker, P. W. Graham, M. Ledbetter, S. Rajendran, and A. O. Sushkov, Proposal for a cosmic axion spin precession experiment (casper), *Phys. Rev. X* **4**, 021030 (2014).
- [33] B. L. Schumaker and C. M. Caves, New formalism for two-photon quantum optics. ii. mathematical foundation and compact notation, *Phys. Rev. A* **31**, 3093 (1985).
- [34] R. Schnabel, Squeezed states of light and their applications in laser interferometers, *Physics Reports* **684**, 1 (2017).
- [35] A. V. Dixit, S. Chakram, K. He, A. Agrawal, R. K. Naik, D. I. Schuster, and A. Chou, Searching for dark matter with a superconducting qubit, *Phys. Rev. Lett.* **126**, 141302 (2021).